Journal of Engineering Science and Technology
Vol. 12, No. 7 (2017) 1740 - 1754
© School of Engineering, Taylor's University

DOUBLE BOSS SCULPTURED DIAPHRAGM EMPLOYED PIEZORESISTIVE MEMS PRESSURE SENSOR WITH SILICON-ON-INSULATOR (SOI)

D. SINDHANAISELVI[1], T. SHANMUGANANTHAM[2]

[1]Department of Electronics and Instrumentation Engineering,
Pondicherry Engineering College, Pondicherry, India
[2]Department of Electronics Engineering, Pondicherry Central University, Pondicherry, India
*Corresponding Author: sindhanaiselvi@pec.edu

Abstract

This paper presents the detailed study on the measurement of low pressure sensor using double boss sculptured diaphragm of piezoresistive type with MEMS technology in flash flood level measurement. The MEMS based very thin diaphragms to sense the low pressure is analyzed by introducing supports to achieve linearity. The simulation results obtained from Intellisuite MEMS CAD design tool show that very thin diaphragms with rigid centre or boss give acceptable linearity. Further investigations on very thin diaphragms embedded with piezoresistor for low pressure measurement show that it is essential to analyse the piezoresistor placement and size of piezoresistor to achieve good sensitivity. A modified analytical modelling developed in this study for double boss sculptured diaphragm results were compared with simulated results. Further the enhancement of sensitivity is analyzed using non uniform thickness diaphragm and Silicon-On-Insulator (SOI) technique. The simulation results indicate that the double boss square sculptured diaphragm with SOI layer using 0.85μm thickness yields the higher voltage sensitivity, acceptable linearity with Small Scale Deflection.

Keywords: Small scale deflection, Shape, Stress, Double boss, Non-uniform thickness, Silicon-On-Insulator.

1. Introduction

Microelectromechanical systems (MEMS) refer to a collection of microsensors and actuators that can sense its environment and have the ability to react to changes

Nomenclatures

E	Young's modulus, GPa
h	Thickness of diaphragm, µm
l	Length of resistor, µm
L	Length of diaphragm, µm
L_{eff}	Effective length of diaphragm, µm
S_{xx}	Longitudinal stress, MPa
S_{yy}	Transverse stress, MPa
y	Center deflection of the diaphragm, µm
y_p	Percentage of deflection, %

Greek Symbols

α	Coefficient of deflection
β	Coefficient of stress
π_l	Piezoresistive coefficient (10^{-11}/Pa)

Abbreviations

CAD	Computer Aided Design
MEMS	Micro Electro Mechanical Systems
SOI	Silicon-On-Insulator
SSD	Small Scale Deflection

in that environment with the use of a microcircuit control. MEMS using micromachining technology emerged as a new discipline and were based on the advancement made in the development of Integrated Circuit fabrication process, by which sensors, accelerometers and actuators were co fabricated in silicon. MEMS devices have been proposed and demonstrated for the applications in such varied fields as microfluidics, aerospace, biomedical, chemical analysis, wireless communications, data storage, display, optics, etc. Among all the MEMS devices, MEMS pressure sensors are most popular both in industrial and commercial applications because silicon micro machined pressure sensors are inherently smaller, lighter and faster than their macroscopic counterparts and are often more precise.

Pressure measurement is certainly one of the most mature applications of MEMS. Pressure is measured using the basic sensing element namely diaphragm, which gives deflection. This is converted into electrical output using a suitable transduction mechanism, namely piezoresistive type. This is most popularly used because it is linear, simple to fabricate and provides temperature compensation using wheat stone bridge arrangement [1]. Low pressure measurement is essential and need to be highly accurate. This low pressure is used in measuring level indirectly such as flash flood level measurement in environmental applications.

In this paper, the double boss sculptured diaphragms with very thin diaphragms were analysed with the performance so that the resulting stress concentrated in relatively localized thin area [2, 3]. The modified analytical modelling [4] is obtained to validate the simulation results. Also, maximum stress concentration region is identified from the longitudinal and transverse stress plot to place polysilicon piezoresistors [5, 6]. The size of piezoresistor and proper positioning of piezoresistor is analysed to improve voltage sensitivity. In addition,

the voltage sensitivity of this double boss sculptured diaphragm is improved by using non uniform thickness and SOI technique is also presented.

2. Structure of the Diaphragm

The typical double boss sculptured diaphragm with the cross sectional top view and back side view is schematically shown in Figs. 1(a) and (b). This is created using bulk micromachining with single crystal silicon by czochrolski process. The diaphragm structure is created with the following material properties : Fracture strength: 7 GPa; Hardness: 850 Kg/mm^2; Young's Modulus (E): 170 GPa; Melting point: 1410°C; Gauge factor:100 to 200; poisson's ratio (ν): 0.3. Silicon satisfies the excellent mechanical and electrical property also it is free of hysteresis and creep [7]. The polysilicon piezoresistors [8] with suitable properties [9, 10], [11, 12] has been considered in this study to realize the piezoresistors using surface micromachining on the top of the diaphragm.

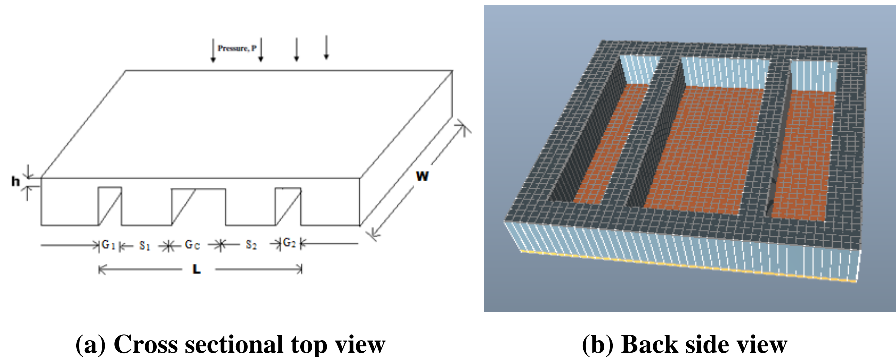

(a) Cross sectional top view **(b) Back side view**

Fig. 1. Typical double boss sculptured diaphragm.

The square diaphragm and rectangular shaped diaphragm were considered due to simplicity in design [13]. Also, the maximum stress at the centre increase and reach a maximum value when the diaphragm is rectangular with its length to width ratio takes a value of two reported in [7]. So the square diaphragm with dimension (500 µm × 500 µm) and rectangular diaphragm with dimension (1000 µm × 500 µm) is considered in this analysis.

3. Mathematical Modelling

The diaphragm is designed with two bosses or two rigids at the center of the bottom. The dimension of the diaphragm is (L µm× W µm× h µm) where L is the length, W is the width and h is the thickness of the diaphragm respectively.

The pressure-deflection model of a flat square diaphragm is given as [14]

$$\frac{Pa^4}{Eh^4} = \frac{4.2}{(1-\nu^2)}\left[\frac{y}{h}\right] + \frac{1.58}{(1-\nu)}\left[\frac{y}{h}\right]^3 \tag{1}$$

where 'P' is the applied pressure in Pa, 'y' is the center deflection of the diaphragm in µm, '$a = L/2$ ' is the half side length of the diaphragm in µm, 'E'

is the young's modulus in GPa, 'h' is the thickness of the diaphragm in μm and 'v' is the poisson's ratio of the diaphragm material.

The first term in the RHS of Eq. (1) represents the Small Scale Deflection (SSD) that is very small compared with the diaphragm thickness (deflection is less than 40% of the diaphragm thickness). Whereas the second term of Eq.(1) gives Large Scale Deflection (LSD), in which deflection is 40% larger than the diaphragm thickness [15].

To achieve Small Scale Deflection, the assumptions of thin plate deflection theory [16] considered are [14, 17],

- The maximum membrane deflection is less than 40% of the membrane thickness.
- Membrane thickness doesnot exceed 10% of the diaphragm length.
- There is no initial stress in the membrane.

The deflection y in the linear region of operation with respect to thickness 'h' is expressed as follows for a square diaphragm

$$y = \frac{\alpha p L^4}{h^3 E} \quad \text{and} \quad \alpha = \frac{(1 - \nu^2)}{4.2 \times 2^4} \text{ is a constant} \tag{2}$$

where 'p' pressure applied, 'L' length of the diaphragm, 'h' thickness of the diaphragm, 'E' young's modulus and α=0.0138 for W/L=1(square).

However, it cannot be used for characterizing the load deflection model of double boss sculptured diaphragms. Hence, it becomes necessary to develop a new model to describe the load deflection response of these sculptured diaphragms [18]. Equation (2) is suitably modified to describe the equations for sculptured diaphragms [17]. When the diaphragm is added with supports in the center, two important changes happen. First the active force loading area decreases. Second the rigidity of the diaphragm is reduced. So incorporating these factors in the modelling is essential to obtain the correct load deflection response. The side length 'L' decides the loading area and the thickness 'h' of the diaphragm decides the rigidity in Eq. (2). Therefore, correctness or validity of the modified analytical model depends on the ability to define the effective side length L_{eff} and effective diaphragm thickness h_{eff} that replace 'L' and 'h' in Eq.(2).

In sculptured diaphragm, double support of required dimension is added to a square or a rectangular diaphragm in the bottom which tends to change the effective 'L_{eff}'. After the introduction of two supports, the square diaphragm is modified length with three rectangle portions on the two sides of the support as shown in Fig. 2 where the displacement takes place on the shaded regions.

Here, S_1, S_2 - support length, G_c - Gap length where deflection occurs (μm), G_1 - length of rectangle formed in the left side by addition of support S_1 (μm), and G_2 is the length of the rectangle formed in the right side by addition of support S_2 (μm), L-total length of the diaphragm and W- total width of diaphragm. Now the change in effective length is given as follows

$$L_{eff} = L - S_1 - S_2 \tag{3}$$

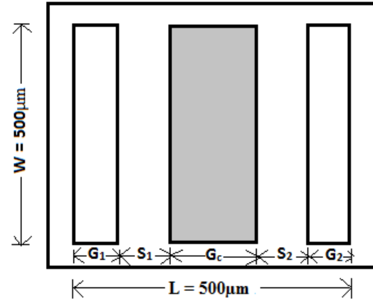

Fig. 2. Bottom view of proposed double boss sculptured diaphragm after addition of two supports.

Based on L_{eff}/W ratio, coefficients α and β is to be selected from Table 1 [14].

Table 1. Coefficients α, β_1 and β_2 with respect to L_{eff}/W ratio.

L_{eff}/W	1	1.2	1.4	1.6	1.8	2.0	∞
α	0.0138	0.0188	0.0226	0.0251	0.0267	0.0277	0.0284
β_1	0.3078	0.3834	0.4356	0.4680	0.4872	0.4974	0.5000
β_2	0.1386	0.1794	0.2094	0.2286	0.2406	0.2472	0.25

Now the deflection given by Eq. (2) is modified as [17]

$$y = y_{eff} = \frac{\alpha P G_1^4}{E h^3} = \frac{\alpha P G^4}{E h^3} \tag{4}$$

where G_1 and G_2 are the length of shaded region where maximum displacement occurs (µm). Therefore $G=G_1=G_2$ (µm). Similarly the effective diaphragm thickness 'h_{eff}' obtained from the new structure after addition of support can be written as

$$h_{eff} = h \tag{5}$$

As there is no change in the thickness, it remains the same. The stress developed in the YY and XX direction in the diaphragm under different applied pressure in the SSD region is given [17] by the Eq. (6)

$$\sigma_{yy} = \beta_1 P \left[\frac{G}{h}\right]^2 \quad and \quad \sigma_{xx} = \beta_2 P \left[\frac{G}{h}\right]^2 \tag{6}$$

where 'P' pressure applied in Pa, 'G' length of the new rectangle in µm and 'h' thickness of diaphragm in µm [17]. The equation for the wheatstone bridge output voltage (V_o) is given as

$$\frac{V_o}{V_b} = \frac{R_4}{R_4 + R_1} - \frac{R_3}{R_2 + R_3} \tag{7}$$

where V_b is bridge excitation voltage. Intially resiatance $R_1 = R_2 = R_3 = R_4 = R_o$ which is the resistance at zero pressure. When pressure is applied, change in resistance with respect to R_o is changed as follows [17]

$$\frac{\Delta R}{R_o} = \frac{(\pi_{11} + \pi_{12} + \pi_{44})\sigma_l + (\pi_{11} + \pi_{12} - \pi_{44})\sigma_t}{2} \tag{8}$$

where σ_l and σ_t are the longitudinal and tensile stress along the diaphragm. In longitudinal orientation, for R_2 and R_4: σ_l=σ_1 MPa and σ_t=σ_2 MPa. In transverse orientation, for R_1 and R_3: σ_l=σ_2 MPa and σ_t = σ_1 MPa.

When pressure applied, the new change in resistance are obtained as follows [17]

$$R_1 = R_3 = R_o(1 + 0.5 \times (1.436 \times \sigma_l - 1.326 \times \sigma_t) \times 10^{-3}) \quad (9)$$

$$R_2 = R_4 = R_o(1 + 0.5 \times (1.436 \times \sigma_t - 1.326 \times \sigma_l) \times 10^{-3}) \quad (10)$$

where R_2 and R_4 are in longitudinal direction and R_1 and R_3 are in transverse direction. Substituting Eqs. (9) and (10) in Eq. (7), the voltage sensitivity is obtained as in Eq. (11)

$$\frac{V_o}{V_b} = \frac{2.762 \times 10^{-3}(\sigma_l - \sigma_t)}{4 + 0.11 \times 10^{-3}(\sigma_l + \sigma_t)} \quad (11)$$

4. Optimized Diaphragm Design

4.1. Diaphragm thickness

The thickness of the sculptured diaphragm is reduced to increase the stress concentration as in Eq. (7). This reduced thickness for the square and rectangular double boss sculptured diaphragm is analyzed by burst pressure approach. Burst pressure P_B is defined as the pressure at which maximum stress σ_{max} on the diaphragm becomes equal to the critical stress σ_c which is actually the yield strength of material [1, 19, 20]. Although, theoretically the fracture or yield strength is 7 GPa for silicon, due to the influence of the diaphragm shape, thickness, lateral dimensions, rupture stress of the material and diaphragm surface roughness, the yield strength has been found considerably lower [21] and its value is equal to1 GPa. P_B is five times the maximum pressure, i.e., $P_B = 5P_{max} = 5(1000) = 5000$ Pa. The thickness is selected in between 0.5 μm to 1 μm to avoid burst condition [14, 17].

4.2. Diaphragm geometry design optimization

The objective of this work is to analyze the positioning of the boss by varying these regions to achieve the maximum deflection sensitivity within the small scale deflection region for square and rectangular diaphragms. The sensor is subjected to pressure on the front side as in Fig. 1. The optimized dimension of double boss sculptured diaphragm with thickness, center deflection and percentage of center deflection at 1000 Pa were given in Tables 2(a) and (b).

From Table 2(a), the double boss square sculptured diaphragm with thickness 1 μm gives the maximum membrane deflection eiether (28%) veryhigh or low(15%). The diaphragm with thickness 0.9 μm gives the maximum membrane deflection eiether (22%) high or verylow(11%). Similarly, the diaphragm with thickness 0.85 μm, gives the maximum membrane deflection eiether (28%) veryhigh or verylow(13%). The diaphragm with thickness 0.8 μm gives the maximum membrane deflection as 17% which is close to small scale deflection.

From Table 2(b), the double boss rectangle sculptured diaphragm with thickness 1 μm gives the maximum membrane deflection eiether (31%) veryhigh

or verylow(9%). The diaphragm with thickness 0.9 µm gives the maximum membrane deflection eiether (48%) veryhigh or low(14%). Similarly, the diaphragm with thickness 0.8 µm, gives the maximum membrane deflection (23%) high. The diaphragm with thickness 0.85µm gives the maximum membrane deflection as 18% which is close to small scale deflection. The center deflection of simulated double boss sculptured diaphragm is shown in Fig. 3.

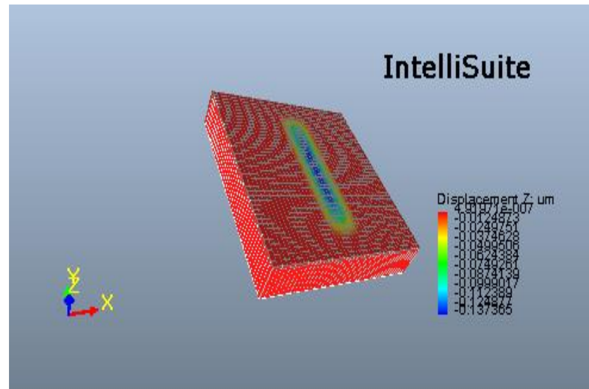

Fig. 3. Simulated double boss sculptured diaphragm with center deflection.

Table 2(a). Double boss sculptured diaphragm (square).

h (µm)	G_1 (µm)	G_2 (µm)	S_1 (µm)	S_2 (µm)	G_c (µm)	y (µm)	y_p (%)
1	40	40	120	120	180	0.148	15
1	40	40	140	140	140	0.277	28
0.9	40	40	130	130	160	0.20	22
0.9	40	40	140	140	140	0.0966	11
0.85	40	40	140	140	140	0.1146	13
0.85	40	40	130	130	160	0.2415	28
0.8	**40**	**40**	**140**	**140**	**140**	**0.137**	**17**
0.8	20	20	160	160	140	0.137	17
0.8	20	20	150	150	160	0.137	17

Table 2(b). Double boss sculptured diaphragm (rectangle).

h (µm)	G_1 (µm)	G_2 (µm)	S_1 (µm)	S_2 (µm)	G_c (µm)	y (µm)	y_p (%)
1	20	20	380	380	200	0.314	31
1	20	20	370	370	220	0.3140	31
1	20	20	390	390	180	0.0943	9
0.9	20	20	380	380	200	0.431	48
0.9	20	20	410	410	140	0.129	14
0.9	100	100	330	330	140	0.13	14
0.85	**20**	**20**	**400**	**400**	**160**	**0.153**	**18**
0.8	40	40	380	380	160	0.18	23

The thickness of the rectangular diaphragm is greater than square diaphragm. The deflection sensitivity of rectangular shape is higher than square diaphragm. This reveals that rectangular diaphragm can be considered as a best suitable shape for sensing low pressures and also can be designed with thickness greater than the square type to avoid breakage of the diaphragm. More than that, when there is packaging constraints limit vis-à-vis the length, there rectangular diaphragms are the suitable choice of shape [21].

4.3. Stress analysis

The stress result of double boss sculptured diaphragm at maximum pressure of 1000 Pa is shown in Figs. 4 with thickness h = 0.8 μm for square diaphragm. The maximum longitudinal stress distribution simulation for a double boss sculptured diaphragm is shown in Fig. 4(a) and maximum transverse stress distribution simulation for a double boss sculptured diaphragm is shown in Fig. 4(b) when uniformly distributed pressure is applied on the top of the diaphragm as in Fig. 4(c).

A closer look at Figs. 4(a), 4(b) and 4(c) clearly shows that the longitudinal stress S_{xx} is tensile (+ve) in nature developed at and around 70 μm from centre of the diaphragm and compressive (-ve) in nature developed at the centre of the diaphragm. The transverse stress S_{yy} is tensile (+ve) in nature developed at and around 70 μm from the centre of the diaphragm and compressive (-ve) in nature at and around the centre of the diaphragm.

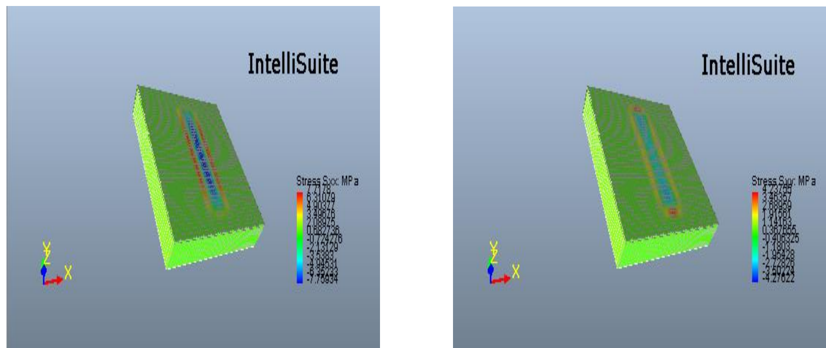

(a) Simulated longitudinal stress **(b) Simulated transverse stress**

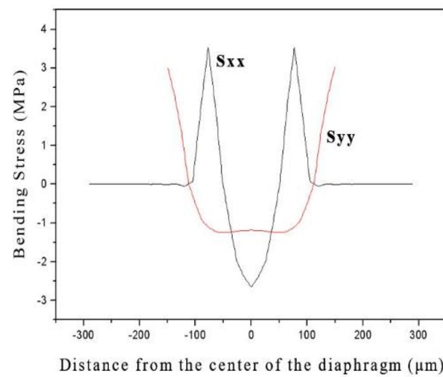

(c) Stress plot

Fig. 4. Stress distribution of double boss sculptured diaphragm.

Similarly, for a rectangular diaphragm longitudinal stress S_{xx} is tensile (+ve) in nature developed at and around 80 µm from centre of the diaphragm and compressive (-ve) in nature developed at the centre of the diaphragm. The transverse stress S_{yy} is tensile (+ve) in nature developed at and around 80 µm from the centre of the diaphragm and compressive (-ve) in nature at and around the centre of the diaphragm.

4.4. Piezoresistive analysis

Four piezoresistors (R_1, R_2, R_3 and R_4) are used in a wheat stone bridge arrangement which gives better temperature compensation. To improve the voltage sensitivity, the four resistors are to be placed in such a way that two resistors (R_1, R_3) experience tensile stress and exhibit increase in their resistance and the remaining two resistors (R_2, R_4) experience compressive stress and exhibit decrease in their resistance from the resistance value measured at no stress condition. Hence to achieve this, the arrangement of resistors is estimated in eight different categories as shown in Fig. 5.

The comparisons of the estimated output voltage with respect to placement patterns of the piezoresistor were given in Table 3.

Table 3. Voltage output versus different placement pattern.

Placement pattern	Output voltage (mV)
a	1.5 mV
b	1.0 mV
c	**3.5 mV**
d	0.8 µV
e	10 µV
f	150 µV
g	100 µV
h	80 µV

Among the eight patterns shown in Fig. 5, pattern (c) gives highest voltage sensitivity of 3.5 mV at 1000 Pa. The size of piezoresistors used to estimate the voltage is 40 µm × 20 µm × 1 µm. It reveals that, pattern (c) is suitable and efficient in extracting the maximum stress into maximum change in resistance which in turn gives the highest voltage sensitivity. The maximum longitudinal stress S_{xx} and transverse stress S_{yy} distribution of double boss sculptured diaphragm referred in Figs. 4 shows that stress is high in the center region as discussed in Section 4.3. So, the four piezoresistors are placed in the shaded region G_c as shown in Fig. 2.

Hence, the polysilicon piezoresistors (R_1, R_2, R_3 and R_4) are placed in the maximum stress regions identified on the diaphragm [6] as shown in Fig. 6. The smith piezoresistive coefficients [22] used in the simulation are as follows: $\pi11 = 6.6\times10^{-11}$ Pa^{-1};$\pi12$ =-1.1×10^{-11} Pa^{-1}; $\pi44$ =138×10^{-11} Pa^{-1}. The dimensions of the piezoresistor used were 16µm×2µm×1µm. The sheet resistance of p-type silicon resistor is 25Ω/square.cm and temperature= 20°C.

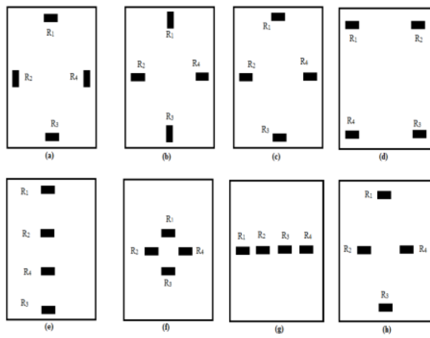

Fig. 5. Different types of arrangement.

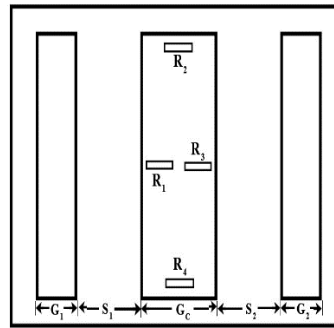

Fig. 6. Piezoresistor placement.

4.5. Electrical output

The electrical output is estimated with the Wheatstone bridge connection using supply voltage of 5V is shown in Figs 7(a) and (b). When the pressure applied to the diaphragm, two resistors undergo longitudinal stress and two resistors undergo transverse stress. Figure 7(a) shows that extraction of electrical output for resistor with stress S_{xx} and Fig. 7(b) for stress S_{yy}. The diagonally opposite resistors produce same electrical output. The electrical output estimated using Eqs. (9), (10) and (11) is given in Tables 4 and 5.

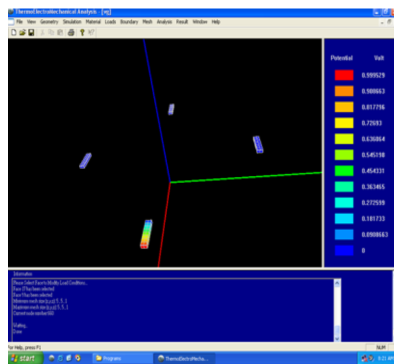

(a) At S_{xx}

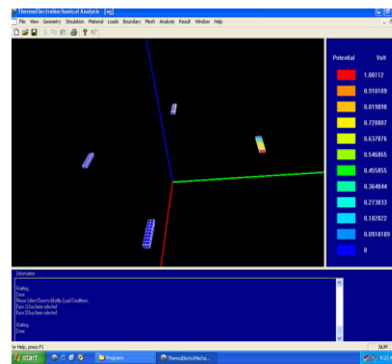

(b) At S_{yy}

Fig. 7. Estimation of electrical output at S_{xx} and at S_{yy}.

4.6. Enhancement of sensitivity

The stress obtained from the previous section is improved by incorporating size of piezoresistor, modifying the thickness of diaphragm and diaphragm with SOI. The piezoresistor size is chosen by estimating the output with **16 μm × 2 μm × 1 μm** [17].

The sensitivity is further enhanced by using SOI structure [19, 20, 23] is created using the surface micromachining technique. The SOI MEMS pressure sensor structure for double boss sculptured diaphragm is shown in Fig.8.

The sculptured diaphragm with SOI is created and its comparison of the improved longitudinal stress, transverse stress, center deflection, percentage of center deflection and voltage output were estimated for square and rectangle diaphragm is given in Tables 4 and 5.

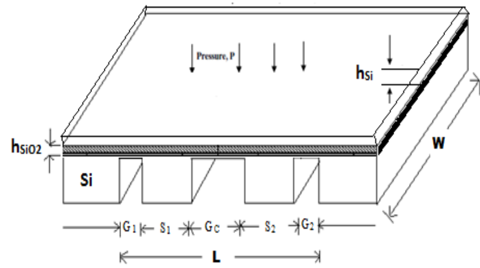

Fig. 8. Double boss sculptured diaphragm with SOI

The double square sculptured diaphragm with SOI yield the higher sensitivity of 4.38 mV and small scale deflection is 28% with silicon diaphragm thickness 0.2µm. The other case yields 6.48 mV but deflection is 52% not satisfying SSD with silicon diaphragm thickness 0.1 µm.

The double boss rectangle sculptured diaphragm with SOI yield the higher sensitivity of 4.84 mV with 30% deflection and 5.16 mV with 42% deflection. The 30% deflection is closer to small scale deflection with 4.84 mV is optimized output using SOI layer to improve sensitivity.

Table 4. Comparison of performance of double boss sculptured diaphragm using different thickness with SOI- square:

Thickness (µm) h=h+h_1		Center deflection (µm)	Percentage of center deflection y_p(%)	S_{xx} (MPa)	S_{yy} (MPa)	V_o (mV/Pa)
h_{Si}= 0.2	**h_{SiO2}=0.6**	**0.237**	**28**	**10.58**	**4.242**	**4.38**
h_S =0.1	h_{SiO2}=0.6	0.377	52	15.69	6.2924	6.48

Table.5. Comparison of performance of double boss sculptured diaphragm using different thickness with SOI - rectangle:

Thickness (µm) h=h+h_1		Center deflection (µm)	Percentage of center deflection y_p(%)	S_{xx} (MPa)	S_{yy} (MPa)	V_o (mV/Pa)
h_{Si}= 0.2	**h_{SiO2}=0.6**	**0.311**	**30**	**11.78**	**4.78**	**4.84**
h_{Si}=0.18	h_{SiO2}=0.6	0.337	42	12.58	5.1	5.16

4.7. Comparison

The double boss sculptured diaphragms of square and rectangle shape were created and their output for the pressure in range of 0-1000 Pa is compared and

analyzed with existing methods [14] and proposed method. The three cases were uniform thickness of diaphragm [14], non-uniform thickness of diaphragm [14] and proposed SOI thickness diaphragm. The measured electrical outputs of square and rectangular with double boss sculptured diaphragm were compared in terms of its thickness, center deflection, stress and sensitivity is given in Table 6.

Table 6. Comparison of performance of proposed diaphragm with existing diaphragm.

Type	Thickness (μm)	Center deflection (μm) with percentage deflection	S_{XX} (MPa)	S_{YY} (MPa)	V_o (mV/V/Pa)
Square Sculptured diaphragm (Existing) [14]	0.8	0.1374 (17%)	7.718	4.238	2.402
Rectangle Sculptured diaphragm (Existing) [14]	0.85	0.1533 (18%)	7.582	4.496	2.130
Square Sculptured with non-uniform thickness (Existing)[14]	0.8	0.1948 (24%)	10.841	5.3824	3.77
Rectangle Sculptured with non-uniform thickness (Existing)[14]	0.8	0.1938 (24%)	10.974	5.408	3.84
Square Sculptured with SOI (proposed)	0.8	0.237 (28%)	10.58	4.242	4.38
Rectangle Sculptured with SOI (proposed)	0.8	0.311 (30%)	11.78	4.78	4.84

The output voltage is compared graphically for various diaphragms are shown in Figs. 9(a) and (b). Figure 9(a) reveals that proposed SOI method with 0.8 μm thickness yields the higher sensitivity of 4.38 mV than the non-uniform thickness

and uniform thickness. The uniform thickness technique yields 2.4 mV with 17% deflection and non-uniform thickness technique yields 3.77 mV with 24% deflection at 1000 Pa.

The square double diaphragm gives higher voltage output but percentage deflection exceeds 30% which shows that SSD is not satisfied. Therefore, double sculptured diaphragm of square type can be chosen when the SSD is not a constraint.

Figure 9(b) reveals that SOI thickness yields the higher sensitivity of 4.84 mV with 30% deflection than the uniform thickness and non-uniform thickness. The rectangle double sculptured diaphragm satisfies the percentage of deflection within SSD range with h = 0.2 µm is used. The non-uniform thickness technique yields 3.842 mV with 24% deflection and uniform thickness yields 2.13 mV with 18% deflection at 1000 Pa.

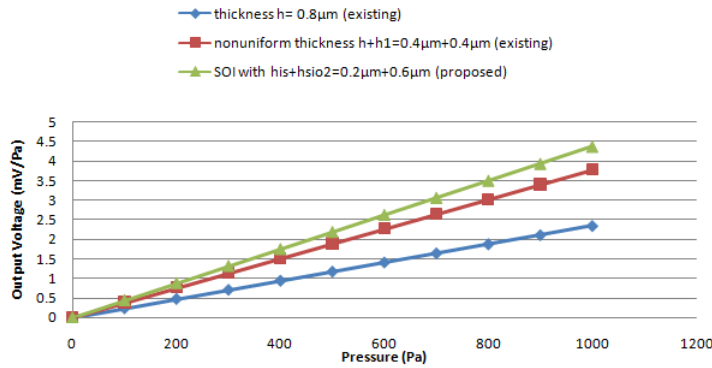

(a) Square

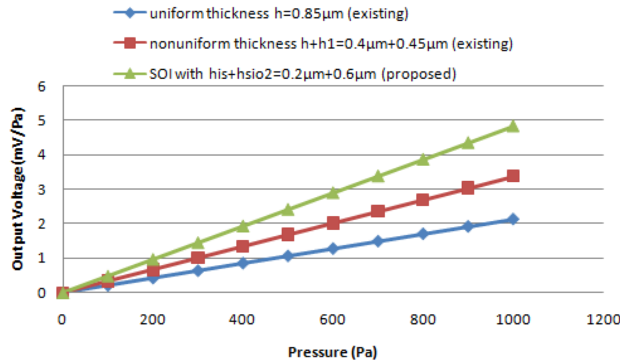

(b) Rectangle

Fig. 9. Comparison of applied pressure versus electrical output of proposed double boss sculptured diaphragm with existing diaphragms.

5. Conclusions

An investigation has been made of the double boss sculptured diaphragm with square and rectangle shapes for low pressure measurement in the range of 0 to 1000 Pa. This is done using analytical equations and Intellisuite MEMS CAD simulation tool. Some concluding observations from the investigation are given below.

- Double boss sculptured diaphragm created with smaller thickness with less than 1 μm reported which satisfies within small scale deflection range is validated to ensure acceptable linearity.
- The comparison of shape shows that the rectangle diaphragm yields higher voltage sensitivity than the square diaphragm.
- Piezoresistor positioning and piezoresistor size were optimized to maximize the voltage sensitivity. Further, sensitivity is enhanced by using SOI technique.
- The double boss rectangular sculptured diaphragm with SOI layer reveals better performance since it provides electrical insulation, reduces noise and increases temperature range.
- Here it shows that increasing the number of supports simultaneously reducing the diaphragm thickness with SOI technique improves the voltage sensitivity.

Acknowledgement

The authors express their sincere gratitude to Dr. R. Joseph Daniel for his encouragement and useful discussions. The authors gratefully acknowledge the support from authorities of National Program on Micro and Smart Systems (NPMASS) Centre of Annamalai University interms of MEMS software design tools.

References

1. Bhat, K.N.; and Nayak, M. (2013). MEMS pressure sensors - an overview of challenges in technology and packaging. *Journal of Institute of Smart Structures and Systems*, 2(1), 39-71.
2. Mallon, J.R.; Pourahmadi, F.; Petersen, K.; Barth T.; Vermeulen, B.T.; and Brezek, J. (1990). Low pressure sensors employing bossed diaphragms and precision etch stopping. *Sensors and Actuators*, A21-A23, 89-95.
3. Sandmaier, H. (1991). Non-Linear analytical modelling of bossed diaphragms for pressure sensors. *Sensors and Actuators*, A25-27, 815-819.
4. Sindhanaiselvi, D.; Ananda Natarajan, R.; and Shanmuganantham, T. (2014). Performance analysis of sculptured diaphragm for low pressure MEMS sensors. *Applied Mechanics and Materials*, 592-594, 2193-2198.
5. Lin, L.; and Yun, Y. (1998). Design, optimization & fabrication of surface micromachined pressure sensors. *Journal of Mechatronics*, 8, 505-519.
6. Sivakumar, K.; Dasgupta, N.; and Bhat, K.N. (2006). Sensitivity enhancement of polysilicon piezo resistive pressure sensors with phosphorous diffused resistors. *Journal of Physics: Conference series*, 34, 216-221.
7. Bhat, K.N. (2007). Reviews - Silicon micromachined pressure sensors. *Journal of the Indian Institute of Science*, 87(1), 115-131.
8. Wang, X.; Li, B.; Russo, O.L.; Roman, H.T.; Chin, K.K.; and Farmer, K. (2006). Diaphragm design guidelines and an optical pressure sensor based on MEMS technique. *Microelectronics Journal*, 37, 50-56.
9. Wisitsoraat, A.; Patthanasetakul, V.; Lomas, T.; and Tuantranont (2007). Low cost thin film based piezo resistive MEMS tactile sensor. *Sensors and Actuators*, 139, 17-22.

10. Clausen, I.; and Sveen, O. (2007). Die separation and packaging of a surface micromachined piezo resistive pressure sensor. *Sensors and Actuators,* A133, 457-466.
11. Aravamudhan, S.; and Bhansali, S. (2008). Reinforced piezo resistive pressure sensor for ocean depth measurements. *Sensors and Actuators*, A142, 111-117.
12. MilonJevti, M.; Miloljub, A.; and Smiliani. (2008). Diagnostic of silicon piezoresistive pressure sensors by low frequency noise measurements. *Sensors and Actuators*, 144, 267-274.
13. Kanda, Y.; and Yasukawa, A. (1997). Optimum design considerations for silicon piezo resistive pressure sensors. *Sensors and Actuators A*, 62, 539-542.
14. Sindhanaiselvi, D.; Ananda Natarajan, R.; and Shanmuganantham, T. (2015). Design and optimization of low pressure sculptured diaphragm with burst pressure, stress analysis and its enhancement. *International Journal of Applied Engineering Research*, 10(24), 21075-21081.
15. Linlin, Z.; Chen, X.; and Guangdi, S. (2006). Analysis for load limitations of square-shaped silicon diaphragms. *Solid State Electronics*, 50, 1579-1583.
16. Timoshenko, S.; and Woinowsky-Krieger, S. (1959). *Theory of plates and shells*, New York: McGraw-Hill.
17. Sindhanaiselvi, D.; Ananda Natarajan, R.; and Shanmuganantham, T. (2015). Analytical modelling of low pressure single boss sculptured diaphragm and its sensitivity enhancement. *ICTACT Journal on Microelectronics*, 1(3), 124-130.
18. Rajavelu, M.; Sivakumar, D.; Joseph Daniel, R.; and Sumangala, K. (2014). Perforated diaphragms employed piezoresistive MEMS pressure sensor for sensitivity enhancement in gas flow measurement. *Flow Measurement and Instrumentation*, 35, 63-75.
19. Narayanaswamy, M.; Joseph Daniel, R.; Sumangala, K.; and Antony Jeyasehar, C. (2011). Computer aided modelling and diaphragm design approach for high sensitivity silicon-on-insulator pressure sensors. *Measurement*, 44, 1924-1936.
20. Narayanaswamy, M.; Joseph Daniel, R.; and Sumangala, K. (2013). Piezoresistor size and placement effect on sensitivity of silicon-on-insulator piezoresistive pressure sensor. *Journal of Instrumentation Society of India*, 43(3), 208-211.
21. Vidhya, B.; and Bhat, K.N. (2012). A comparison of burst strength and linearity of pressure sensors having thin diaphragms of different shapes. *Journal of Institute of Smart Structure Systems*, 2(2), 18-26.
22. Smith, C.S. (1954). Piezo resistance effect in germanium and silicon. *Physical Review*, 94, 42-49.
23. Dimitropoulos, P.D.; Kachris, C.; Karampatzakisa, D.P.; and Stamoulis, G.I. (2005). A new SOI monolithic capacitive sensor for absolute and differential pressure measurements. *Sensors and Actuators*, A123-124, 36-43.